Journal of Groundwater Science and Engineering
ISSN 2305-7068
Indexed by ESCI CABI CSA Scopus GeoRef AJ CNKI

Determination of groundwater solute transport parameters in finite element modelling using tracer injection and withdrawal testing data

Van Hoang Nguyen

Citation:
Nguyen VH. 2021. Determination of groundwater solute transport parameters in finite element modelling using tracer injection and withdrawal testing data. Journal of Groundwater Science and Engineering, 9(4): 292-303.

View online: https://doi.org/10.19637/j.cnki.2305-7068.2021.04.003

Journal homepage: http://gwse.iheg.org.cn

Determination of groundwater solute transport parameters in finite element modelling using tracer injection and withdrawal testing data

Van Hoang Nguyen*

Institute of Geological Sciences-Vietnam Academy of Science and Technology, Hanoi, Vietnam.

Abstract: The groundwater tracer injection and withdrawal tests are often carried out for the determination of aquifer solute transport parameters. However, the parameter analyses encounter a great difficulty due to the radial flow nature and the variability of the temporal boundary conditions. An adaptive methodology for the determination of groundwater solute transport parameters using tracer injection and withdrawal test data had been developed and illustrated through an actual case. The methodology includes the treatment of the tracer boundary condition at the tracer injection well, the normalization of tracer concentration, the groundwater solute transport finite element modelling and the method of least squares to optimize the parameters. An application of this methodology was carried out in a field test in the South of Hanoi city. The tested aquifer is Pleistocene aquifer, which is a main aquifer and has been providing domestic water supply to the city since the French time. Effective porosity of 0.31, longitudinal dispersivity of 2.2 m, and hydrodynamic dispersion coefficients from $D = 220$ m^2/d right outside the pumping well screen to $D = 15.8$ m^2/d right outside the tracer injection well screen have been obtained for the aquifer at the test site. The minimal sum of squares of the differences between the observed and model normalized tracer concentration is 0.001 19, which is corresponding to the average absolute difference between observed and model normalized concentrations of 0.035 5 (while 1 is the worst and 0 is the best fit).

Keywords: Groundwater solute transport; Tracer injection; Effective porosity; Longitudinal dispersivity; Flow distortion coefficient; Normalized concentration

Received: 05 May 2021/ Accepted: 09 Oct 2021

Introduction

Solute transport parameters of aquifer formations are important for many environmental applications and modelling processes such as transport of chemicals and fertilizers in agricultural soils, salt water intrusion into fresh aquifers, desalinization of salinized aquifers, groundwater (GW) contamination, remediation of contaminated aquifers etc. Therefore, GW solute transport parameter identification is very essential in soil and GW environmental science and engineering. The success of the GW solute transport parameter identification in terms of both financial constraints and reliable analysis certainty is a high expectation and wish of the GW hydrologists.

There are two groups of experiments for determining these parameters such as laboratory and field tracer experiments. The laboratory tracer experiments usually used the prototype configurations which provide essential one-dimensional or two-dimensional flow with uniform flow velocity and determined boundary conditions which allow analytical analyses in case of uniform soil column, or numerical analyses in case of multi-layer soil column (Zhou, 2002; Sharma et al. 2014). In more general situations, the field tracer experiments can be conducted in a variety of flow conditions, including steady-state flow (either induced or ambient) and transient flow. Analytical solutions could be available only under steady flow and in homogeneous aquifer in terms of hydraulic properties (aquifer thickness, hydraulic conductivity, porosity, etc.) and dispersion properties. Otherwise, numerical methods need to be used to interpret test results for the determination of dis-

*Corresponding author: Van Hoang Nguyen, *E-mail address*: N_V_Hoang_VDC@yahoo.com

DOI: 10.19637/j.cnki.2305-7068.2021.04.003

Nguyen VH. 2021. Determination of groundwater solute transport parameters in finite element modelling using tracer injection and withdrawal testing data. Journal of Groundwater Science and Engineering, 9(4): 292-303.

persivity and effective porosity. The most popular method of conducting tracer experiments involves one or more tracer injection wells and multiple withdrawal wells (Shook et al. 2004).

There are numerous studies both on laboratory and field tracer experiments and analyses, of which some are shortly described in chronological sequence as follows. Klotz et al. (1980) carried out laboratory and field tracer tests to determine longitudinal dispersion, the results of which are compared and correlated to translate the laboratory results to the field conditions based on the sediment properties. Barone et al. (1992) conducted a series of laboratory tracer column tests with undisturbed clayey soils and found that diffusion coefficient is significantly influenced by adsorption of the tracer, however the tests may provide estimates on the upper and lower bounds of soil diffusion coefficient. Welty and Gelhar (1994) considered non-uniform flow effects in determination of field-scale values of longitudinal dispersivity from tracer tests in aquifers in convergent radial flow, divergent radial flow, and doublet (a test using tracer injection well and withdrawal well) with pulse and step tracer inputs. Glen et al. (1999) carried out three doublet tracer tests at spacings of 30.5, 91.4 and 183.0 meters in approximately 40-meter-long open boreholes using a pulsed bromide injection and both analytical and numerical simulations were used to determine the longitudinal dispersivity and effective porosity of fractured aquifer in Newark basin, New Jersey, USA. Yan et al. (2019) carried out a series of laboratory tracer column experiments for the determination of hydrodynamic dispersion coefficient in the form of a power of 1-2 of the seepage velocity, as the studies of Rifai et al. (1956) and others showed that the hydrodynamic dispersion coefficient is a power of slightly greater than one of the seepage velocity.

The preference of laboratory or field tracer tests, besides various study constraints such as budget and time, depends upon the scale of the study area. The mean travel distance of 2-4 m for a tracer solute or a contaminant is defined as a local scale by Fried (1975), for which the laboratory tracer tests are appropriate. The mean travel distances 4-20 m, 20-100 m and greater than 100 m are defined as global scale 1, scale 2 and scale 3, respectively (Fried, 1975), for which field tracer tests are preferable. According to Gelhar et al. (1992), high-reliability dispersivity data obtained from field tracer tests should meet the following criteria: 1) carried out in ambient flow, diverging radial flow or injection-withdrawal wells; 2) well defined tracer input; 3) conservative tracer; 4) appropriate measurements of tracer concentration; 5) appropriate parameter analysis (breakthrough curve analysis in case of ambient flow and radial flow; method of spatial moments in case of ambient flow; numerical method). Therefore, the tracer test using injection-withdrawal wells along with the four remaining criteria is considered in this study. Analytical analyses of the tracer injection-withdrawal testing data can only be done for specific conditions, including steady state flow and certain injection schemes (slug injection or constant continuous injection) and are approximate solutions using average pore water velocity with three parameter-variables: Longitudinal dispersivity, average hydrodynamic dispersion coefficient and effective porosity (Shook et al. 2004; Gutierrez et al. 2013). Numerical models have become standard methods of interpreting tracer tests (Shook et al. 2004).

The parameter analysis used in this study is the Galerkin finite element (FE) method which is applied to the advection-dispersion equation describing the solute transport by GW. Considering a two-dimensional plane view, since the groundwater flow and solute transport have a radial diverging-converging flow nature, two-dimensional numerical model would not be able to cope with this advanced radial nature. However, the one-dimensional model domain along the line connecting the tracer injection and withdrawal wells would represent the main solute transport from tracer injection well to withdrawal well properly. Besides, from the practical point of view in applications of numerical modelling, the best available models do not have to be more sophisticated models for solving a specific problem as they do not necessarily give more accurate results (Dong, 1998). Therefore, an adaptive methodology of determining GW solute transport parameters using tracer injection-withdrawal test data is worthwhile to be developed. The paper presents the development of a methodology which includes the treatment of the tracer boundary condition at the tracer injection well, the normalization of tracer concentration, the GW solute transport FE modelling and the optimization of parameters using the method of least squares. The application of the developed methodology is illustrated through sodium chloride injection-withdrawal test in Pleistocene aquifer in the northern area of Hanoi city.

1 Local hydrogeological units, testing wells' scheme and testing data

1.1 Hydrogeological units

Groundwater from Pleistocene aquifer in Hanoi city has been exploited for different purposes since the late of 19th century and is still a predominant source of domestic water for Hanoi city (Honjo et al. 1997; Keisuke et al. 2017). As a result, the cone of GW level depression is getting larger and approaching the boundary of brackish groundwater in the south of Hanoi city (Trieu Duc Huy, 2015)①. The salt solution (hereafter called a tracer or solute in concrete context) injection testing at the experimental well system CHN5 had been conducted to determine the solute transport parameters of the lower Pleistocene aquifer, namely the effective porosity n_{eff} and longitudinal dispersivity a_L. These parameters are needed for the predictive modeling of the contaminant transport in the aquifer, including the brackish groundwater intrusion from Southern Hanoi (Fig. 1) towards the center of Hanoi city where the GW pumping fields are located. Besides the salt intrusion, the aquifer is also vulnerable to arsenic as the concentration is high in some parts of the Pleistocene aquifer and the above Holocene aquifer (Do Van Binh, 2013; Martyna et al. 2021). Fig. 2 shows the boundary between the fresh and brackish GW in the Pleistocene aquifer in Southern Hanoi.

The following hydrogeological units are present in the study area from top to bottom:

-Holocene aquifer (qh): covering the whole area. The aquifer is between the depths of 4-5 m and 40-44 m, mainly consisting of sands and silty sands. Overlying the aquifer is a low-permeability layer with clay and silty clay of 2.8-5.0 m in thickness.

-Vinh Phuc formation (Q_1^3vp): With low permeability and thickness of 2-8 m. This layer is present throughout the study area.

-Pleistocene aquifer (qp): occurring between the depths of 43-52 m and 64-69 m. This aquifer is usually divided into two sub-aquifers: The upper Pleistocene aquifer (qp_2) and the lower Pleistocene aquifer (qp_1), separated by an impermeable layer of clay. The aquifer consists of pebbles and gravels with sands. The wells in the aquifer have pumping rates from 6.06 L/s to 12.33 L/s. The estimated transmissivity is from 80 m^2/d to 630 m^2/d.

-Fractured Neogene aquifer (n_2): underlying the sub-aquifer qp_1, this aquifer consists of sandstone and conglomerate.

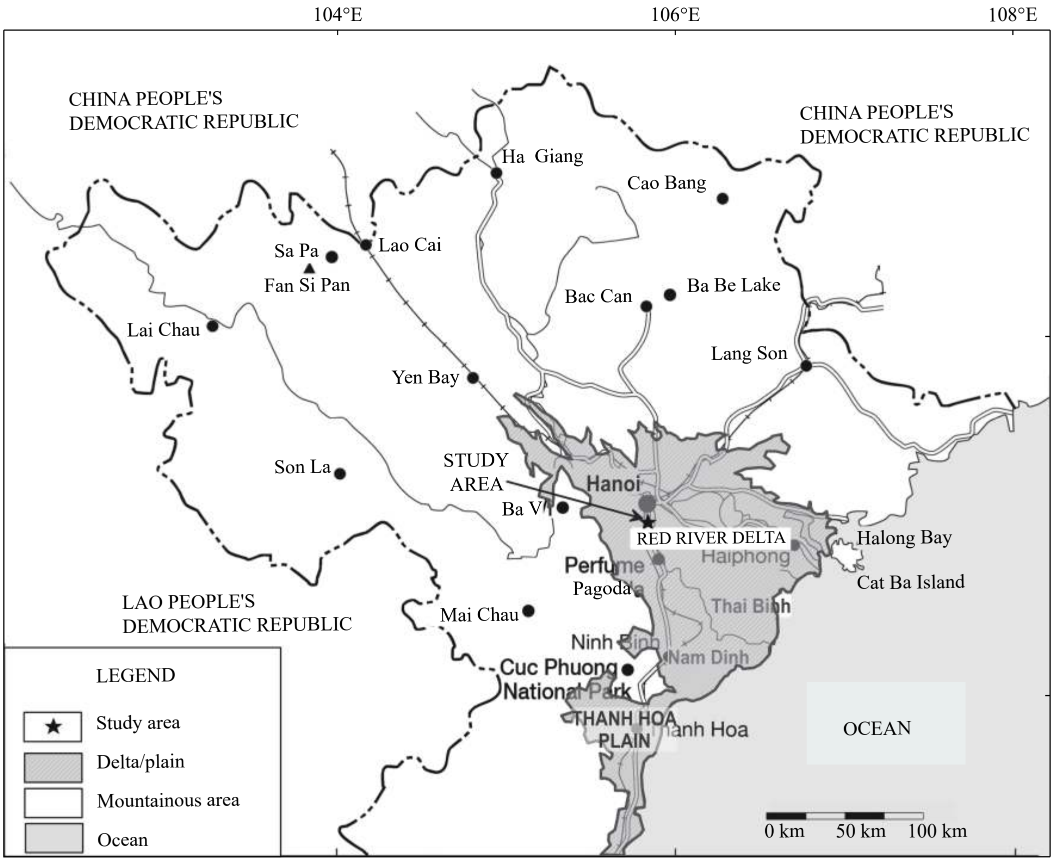

Fig. 1 Location map of the study area

①Trieu Duc Huy (Project head). 2015. Groundwater protection in large cities (city: Hanoi). Vietnam National Center for Water Resources Planning and Investigation-MoNRE.

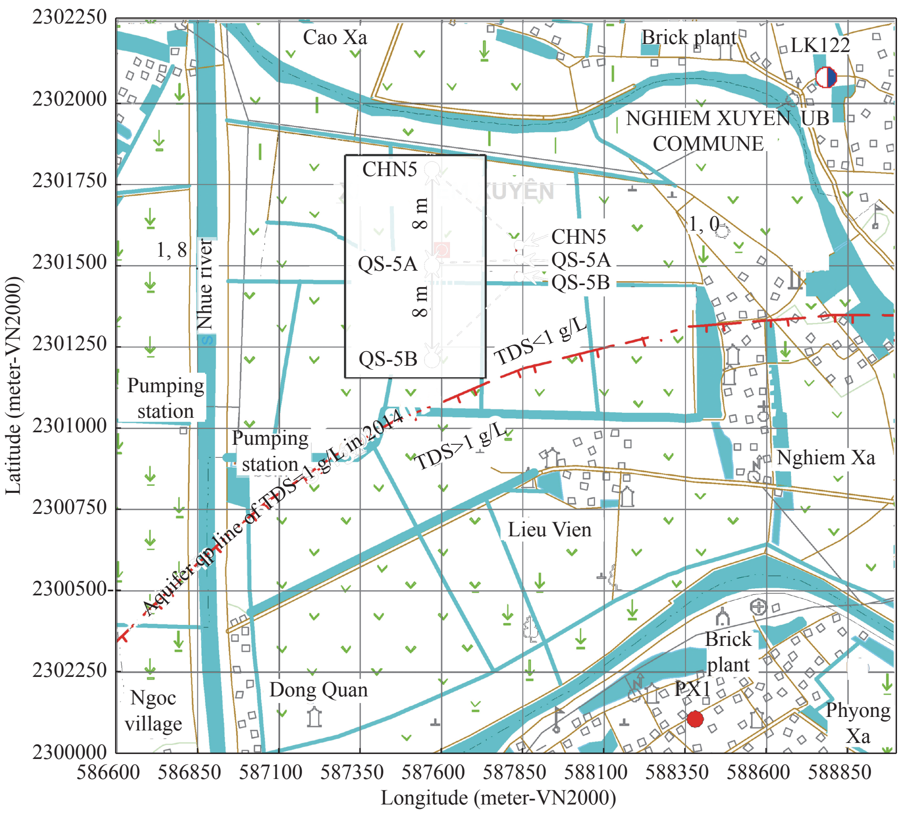

Fig. 2 Testing wells' scheme, location and Pleistocene aquifer on fresh-brackish boundary

1.2 Scheme of testing wells and testing data

Based on the average thickness and effective porosity of the aquifer (qp) in the testing area (Table 1) and the approved testing time in the project proposal, the distances between the testing wells have been determined as 8 m as shown in Fig. 2 and Fig. 3. The wells include the central pumping well CHN5, the tracer solution injection well QS-5, and the observation well QS-5B for monitoring the possible intrusion of the brackish GW. The hydrogeological section through the wells has been constructed from the drilling data (Fig. 3) and well log (Fig. 4) of the central well CHN5. The central well has a diameter of 0.168 m and both observation wells have a diameter of 0.09 m.

Table 1 Estimated hydraulic parameters of the Pleistocene aquifer and well information in the testing area

Well	Aquifer	Well's capacity (L/s)	Drawdown (m)	Hydraulic conductivity (m/d)	Transmissivity (m^2/d)
LK114	qh	3.33	2.54	12.19	210
LK140A	qp	13.20	7.88	20.71	290
LK141	qp	12.62	1.03	70.00	1 610
LK119A	qh	3.84	1.15	9.20	260
LK120	qp	11.48	0.78	152.00	1 670
LK121	qp	12.33	2.05	36.82	630
LK122	qp	6.06	15.17	12.80	80
LK104	qp	6.67	2.35	22.68	410
LK101	qp	9.09	5.04	23.14	240
LK102	qp	12.50	0.87	58.05	1 680
LK103	qh	8.33	3.47	9.70	330
LK129	qp	21.79	1.09	83.53	2 510
LK110	qp	7.82	4.04	18.28	210
LK130	qh	0.40	16.19		

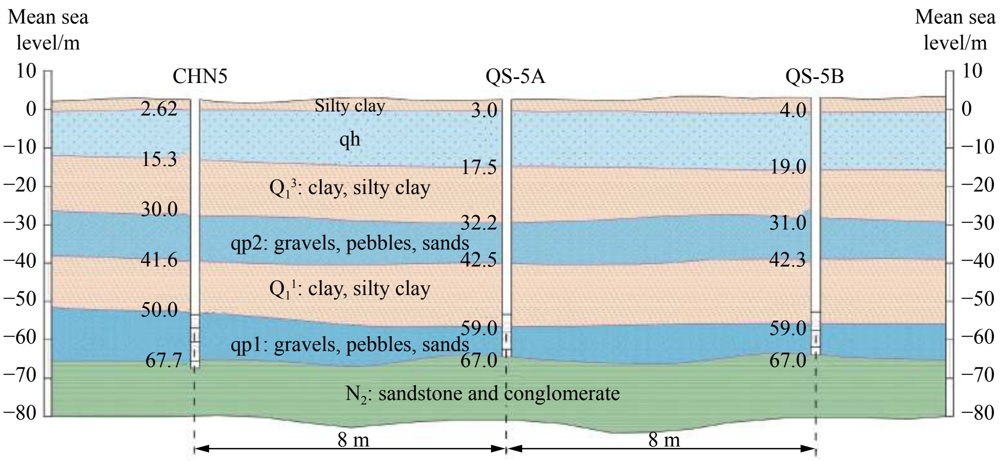

Fig. 3 Hydrogeological section through the testing wells

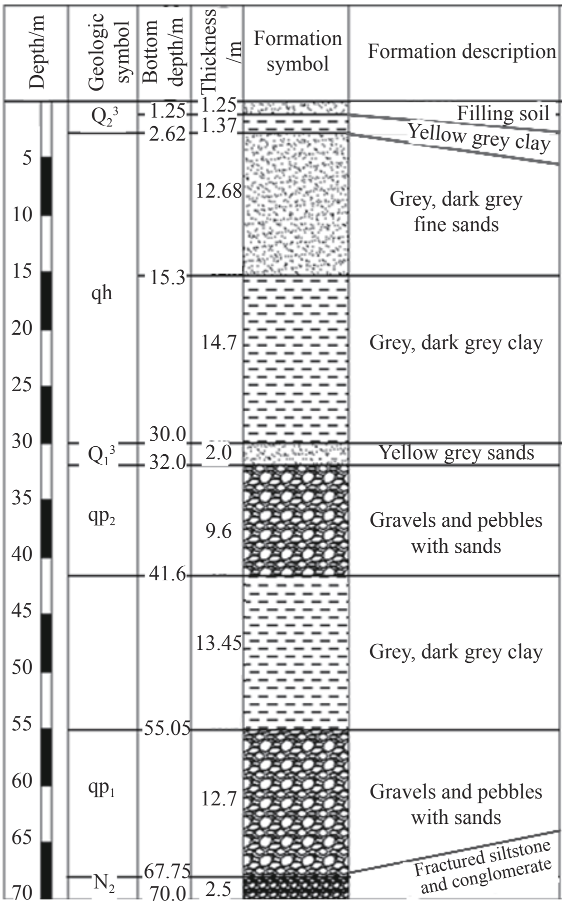

Fig. 4 Well log of central well CHN5

The aquifer under testing is the sub-aquifer qp_1 in the depth from 55.05 m to 67.75 m, i.e. the aquifer thickness is 12.7 m (Fig. 4). The testing time is 60 hours. The pumping out and tracer solution injection started at the same time. Pumping rate is 2 592 m^3/d (30 L/s) and injection rate is 60.48 m^3/d (0.7 L/s), which is equivalent to 2.33% of the pumping rate. With these pumping and injection rates, the possible maximal total dissolved solids (TDS) of the pumped out water would be 1.675 g/L, which has a TDS increased 228% since the natural GW of the sub-aquifer qp_1 at the testing site has TDS of 0.51 g/L and the injection salt solution is prepared by adding 5 g of salt in a litter of the natural GW. If the flow distortion coefficient α_w is very high, for example 20, then the TDS of the pumped out water would be 0.568 g/L which is equivalent to TDS increase of 11.4%, which is big enough to analyze the TDS breakthrough curve. The TDS of the water is always referred to water at the temperature of 25℃. The salt solution in the injection well is constantly well mixed with the well water.

1.3 Obtained testing data

The testing started at the 8 AM the 11th Oct. 2015. The TDS of the water inside the injection well is plotted against the full testing time in Fig. 5 and that of the pumped out water is plotted in Fig. 6.

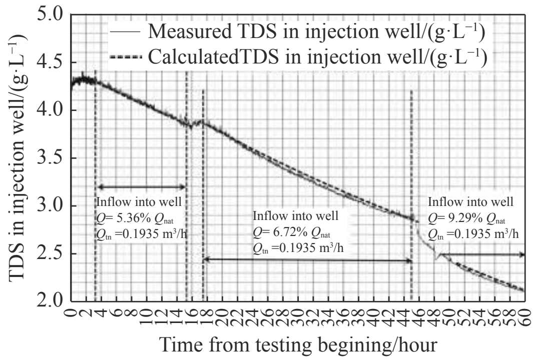

Fig. 5 GW TDS in the injection well

1.4 Boundary condition at the outside injection well

Boundary condition of solute transport at the injection well can be interpretated differentially by diff-

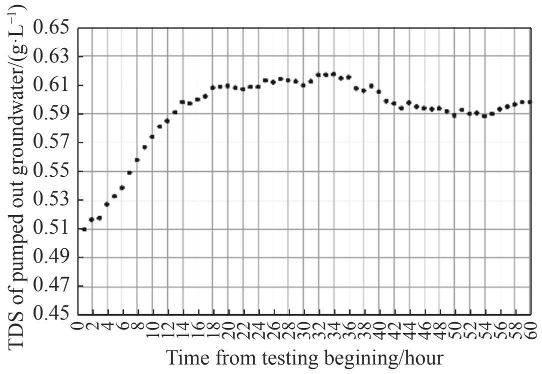

Fig. 6 TDS of the pumped out GW

erent researchers in order to solve the problem.

According to Novakowski (1992), the flow rate of the solute mass in GW around the injection well can be considered as a specified value equal to the dispersion term and advection term. However, in the case of injection borehole with filter pack, both the dispersion and advection terms are unknown. This type of boundary condition can' t be directly used in this case.

According to Drost et al (1968), the solute concentration of GW around the injection well depends upon the flow rate through the well towards the pumping well and the solute solution injection regime, and can be considered as a specified solute concentration. The specified solute concentration outside the screen of the injection well may be determined as follows.

For the case of the injection well does not cause any disturbance of the GW flow as that there is no well, the GW flow through the entire injection well section (Q_{nat}) (Fig. 7) is determined by the following equation:

$$Q_{nat} = \frac{Qr_I}{\pi m r_L n_{eff}} \quad (1)$$

Where: Q is the pumping rate from the central pumping well (M^3/T); Q_{nat} is the flow through the injection well section (M^3/T); r_I is the radius of the injection well (L); r_L is the distance between the central pumping well and injection well (L); m is the aquifer thickness (L); n_{eff} is the effective porosity of the aquifer.

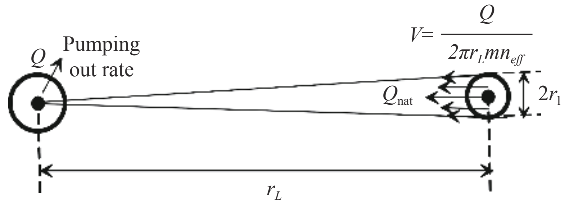

Fig. 7 GW flow through the injection well section

With the pumping rate of 2 592 m^3/day and other relevant data as given above, the natural flow rate through the injection well section is Q_{nat} = 0.193 5 m^3/h. Due to the additional hydraulic resistance from the injection well, the actual flow rate through the well is always smaller than the natural flow rate given in Equation (1) and Fig. 7 (Drost et al. 1968). The distortion flow coefficient α_W is defined as the ratio between the flow rates through the injection well section with and without its presence ($\alpha_w = Q_{nat}/Q_{well}$) (Drost et al. 1968; Hall, 1996). As the TDS of the GW inside the injection well is measured during the testing, the GW flow rate Q_{well} into and out the injection well can be determined by the following balance of the mixing of two volumes of water with two known TDS values: known volume of water inside the injection well with known TDS equal to C^1_{well} at time t_1, TDS equal to C^2_{well} at time $t_2 = t_1 + \Delta t$ and TDS of the natural GW equal to C_{nat}:

$$C^2_{well} = \frac{C^1_{well}(V_{well} - \Delta t Q_{well}) + C_{tn} Q_{well}}{V_{well}} \quad (2)$$

Then the flow distortion coefficient α_w is the ration between Q_{well} and Q_{nat}.

By Equation (2) using the obtained measured TDS inside the injection well, the following results have been obtained (Fig. 5):

-From the 3.5th hour to the 15.5th hour: Q_{well} = 0.010 4 m^3/h (α_w = 18.66);

-From the 17.5th hour to the 45th hour: Q_{well} = 0.013 0 m^3/h (α_w = 14.88);

-From the 49th hour to the end of the testing: Q_{well} = 0.017 8 m^3/h (α_w = 10.76).

It is worthwhile to note that Brouyère (2003) had obtained α_w=11.50 for a well of radius 0.025 m in the study, which is close to the value (α_w = 10.76) in the last stage of the testing in this study.

2 Proposed methodology for determining effective porosity and longitudinal dispersivity

2.1 Interpretation of the obtained tracer injection testing data

The TDS breakthrough curves for injection well and pumped out water are combined into one plot in Fig. 8. The TDS of the GW in the pumping well started to increase very early since the 2nd hour and almost linearly increased until the 13th hour. The curve shows a stabilization trend at the 18th hour, which may indicate that the advection time of the solute from the injection well to the pumping well is around 18 hours. After 18 hours the solute concentration is fluctuated till the 36th hour due to the

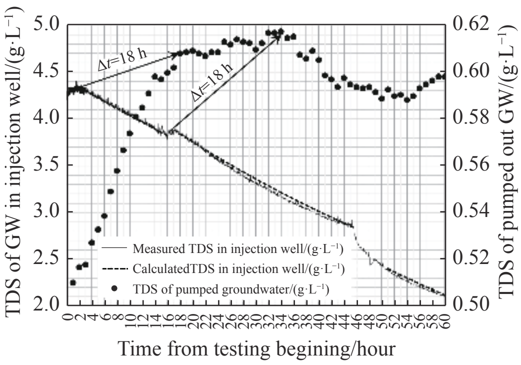

Fig. 8 Breakthrough curves of TDS in injection and pumping wells

most probable reason that the solute injection rate was not stable all the time. The solute concentration then decreases from the 36th hour to 55th hour.

In the injection well, the solute concentration has an increasing trend from the 16th hour, which is corresponding to the maximal solute concentration in the pumping well at the 34th hour and the advection time from the injection well to the pumping well of 18 hours. The advection time of 18 hours is used in the identification of effective porosity and the longitudinal dispersivity in the following part of the paper.

2.2 FE modeling for determination of effective porosity and longitudinal dispersivity

The Galerkin FEM with linear shape functions and central time scheme with time step Δt_n (Zienkiewicz and Morgan, 1983) has been applied to the partial differential equation describing the solute transport by advection-dispersion in one dimensional space between the injection well and pumping well. The time step and element size have been selected based on the criteria on Peclet and Courant numbers (Huyakorn and Pinder, 1983). The GW flow and solute transport FE modeling software was developed within the NOFOSTED research project headed by Nguyen Van Hoang (2018). The GW solute transport FEM program had been embedded with the algorithm of the method of least squares for parameter identification.

The main mechanism of solute transport by GW in the zones between the injection and pumping wells have been identified and described by Zlotnik and Logan (1996). The width W between the capture zone in the upstream of the injection well and the supply zone to the pumping well by Drost et al (1968) has a value not greater than two times of injection well's diameter if the permeability of the disturbed aquifer around the injection well is smaller than that of the natural aquifer. This always happens in the practice of drilling and construction of GW monitoring wells. Therefore, for the testing scheme in this study, the maximal width of the solute transport zone is about 0.2 m, which is significantly smaller than the distance between the injection and pumping wells. Therefore, one-dimensional modelling of the solute transport may be applied for the purpose of transport parameter identification.

In the testing, the solute concentration of the pumped-out GW is measured, however, the modelling can provide the GW concentration only at the edge of the pumping well screen. As a rule, the concentration in the pumped out GW is exactly linearly proportional to the solute concentration right outside the pumping well. Therefore, normalized solute concentrations shown in Fig. 9 for the pumped out GW and GW right outside the pumping well may be used for the purpose of parameter identification. Theoretically, the two normalized solute concentrations are identical. Taking notations of the solute concentration of pumped out GW as C_{pum} with the maximal value C_{pummax} and minimal C_{pummin} (Fig. 9a), and correspondingly those for the solute concentration at the edge of the pumping well in the model as C_{1Dmax} and C_{1Dmin}, the normalized solute concentrations in the pumped out GW and GW in the edge of the pumping well are as follows:

$$C = \frac{C_{pum} - C_{pum\min}}{C_{pum\max} - C_{pum\min}};\ C = \frac{C_{1D} - C_{1D\min}}{C_{1D\max} - C_{1D\min}} \quad (3)$$

The transformation of absolute solute concentration (Fig. 9a) into normalized solute concentration is illustrated in Fig. 9b.

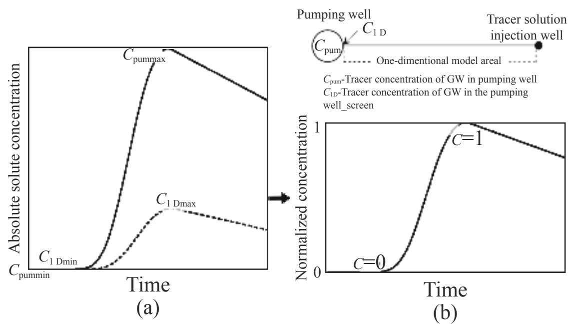

Fig. 9 The transformation of absolute solute concentration into normalized solute concentration

2.3 Parameter identification results

Since the Pleistocene aquifer consists of coarse sands, gravels and pebbles, the adsorption or desorption of salt may be negligible, i.e. the retardation coefficient is assumed as 1.0 in the identification of effective porosity and dispersivity.

In accordance with the results of pumping test of the sub-aquifer qp_1 (Tong Thanh Tung, 2015)① the sub-aquifer qp_1 is a leaky confined aquifer thanks to the contact with the Neogene (n_2) fractured sandstone and conglomerate aquifer below. For a leaky confined aquifer, the early pumping data are entirely representing the confined aquifer without leakage effect (Fetter, 2001). As the data in Fig. 10 shows, during the first 60 minutes of pumping, the slope of the drawdown curve is equal to 0.36 which is two times greater than the average slope over the whole pumping time. It means that the leakage from the Neogene aquifer provides around 50% of the pumping rate during the later pumping time. Therefore, the pumping rate Q should be decreased to the half value in the calculation of the sub-aquifer qp_1, which would result in an effective porosity of 0.390 2. The effective porosity shall be further refined together with the longitudinal dispersivity identification by the FE modeling.

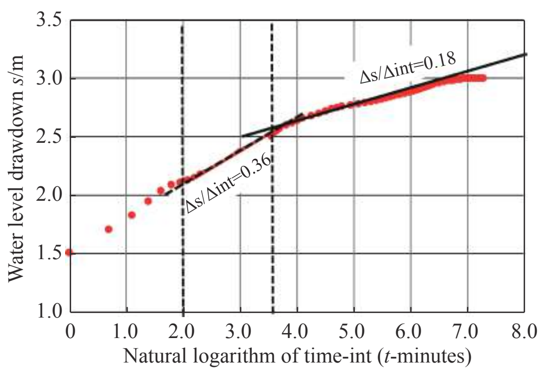

Fig. 10 Drawdown curve of the pumping well QS-5A 13 (Tong Thanh Tung, 2015)

Effective porosity and longitudinal dispersivity have been identified and refined by the algorithm of least squares between the observed and modelled concentrations. The FE modeling of the advection-dispersion solute transport by GW was provided by the Governmental project supported by NAFOSTED-MOST (Nguyen Van Hoang, 2018). The input ranges of the effective porosity and longitudinal dispersivity are 0.20-0.40 and 1.0-3.4 m, respectively. The identification analysis yielded the effective porosity of 0.31 and longitudinal dispersivity of 2.20 m which are corresponding to the least squares of 0.001 19. The detailed results of the identification modeling are presented in Table 2 and Fig. 11.

The absolute and normalized solute concentrations in the pumped GW and at the pumping well screen corresponding to the identified effective porosity and longitudinal dispersivity which had the minimal least squares are presented in Fig. 12 and Fig. 13, respectively. With the identified effective porosity and longitudinal dispersivity the hydrodynamic dispersion is estimated as from D = 220 m^2/d at the pumping well screen to D = 15.8 m^2/d at the injection well screen with the minimal average least squares of 0.001 19, which is corresponding to average difference between the observed and model normalized concentration of 0.035 5 while the normalized concentration range is 0-1. The model result shows that the maximal solute concentration outside the pumping well screen is 6.1 times greater than the solute concentration of the pumped water (Fig. 12).

2.4 Parameter identification uncertainty

The model used in the parameter identification is a lumped-parameter model in which spatial variations of parameters are ignored and the aquifer is described by fitted parameter values (effective porosity and dispersivity). Therefore, the estimated parameters' uncertainty is due to the possible variation of the parameters in space and even in directional orientation.

The second possible factor affecting the parameters' uncertainty is the assumption of no adsorption-desorption in the aquifer as the formation mainly consists of coarse sands, gravels and pebbles. However, the formation would not be completely free of organic maters and clay minerals.

The third possible factor affecting the parameters' uncertainty is that the GW velocity in the solute transport was calculated for a non-leaky confined aquifer. The tested aquifer qp_1 is overlain by a layer of clay and silty clay and underlain by the Neogene sandstone and conglomerate which may provide some leakage to the tested aquifer, and therefore may change the GW velocity.

The hydrodynamic dispersion coefficient used in the parameter analysis is a linear function of seepage velocity. However, the hydrodynamic dispersion coefficient may be in the form of a power function of seepage velocity as addressed early (Rifai et al. 1956; Yan et al. 2019).

Other factor of the parameters' uncertainty is the

①Tong Thanh Tung. 2015. Specialized report: Interpretation and analysis of aquifer parameters for pumping test at group-well test CHN5 in Nghiem Xuyen-Thuong Tin-Hanoi. Project "Groundwater protection in large cities (city: Hanoi)". Vietnam National Center for Water Resources Planning and Investigation-MoNRE.

Table 2 The average least squares and corresponding effective porosity and longitudinal dispersivity

n_{eff}	a_L (m)	Average least squares	n_{eff}	a_L (m)	Average least squares	n_{eff}	a_L (m)	Average least squares
0.26	1.80	0.003 728	0.29	2.70	0.002 551	0.33	2.30	0.001 569
0.26	1.90	0.004 006	0.29	2.80	0.002 734	0.33	2.40	0.001 429
0.26	2.00	0.004 286	0.29	2.90	0.002 919	0.33	2.50	0.001 329
0.26	2.10	0.004 565	0.29	3.00	0.003 104	0.33	2.60	0.001 264
0.26	2.20	0.004 840	0.30	1.80	0.001 288	0.33	2.70	0.001 227
0.26	2.30	0.005 111	0.30	1.90	0.001 231	0.33	2.80	0.001 212
0.26	2.40	0.005 377	0.30	2.00	0.001 222	0.33	2.90	0.001 217
0.26	2.50	0.005 636	0.30	2.10	0.001 253	0.33	3.00	0.001 239
0.26	2.60	0.005 889	0.30	2.20	0.001 314	0.34	1.80	0.004 463
0.26	2.70	0.006 136	0.30	2.30	0.001 399	0.34	1.90	0.003 792
0.26	2.80	0.006 375	0.30	2.40	0.001 500	0.34	2.00	0.003 239
0.26	2.90	0.006 608	0.30	2.50	0.001 615	0.34	2.10	0.002 785
0.26	3.00	0.006 832	0.30	2.60	0.001 743	0.34	2.20	0.002 414
0.27	1.80	0.002 522	0.30	2.70	0.001 880	0.34	2.30	0.002 113
0.27	1.90	0.002 746	0.30	2.80	0.002 023	0.34	2.40	0.001 871
0.27	2.00	0.002 980	0.30	2.90	0.002 172	0.34	2.50	0.001 679
0.27	2.10	0.003 220	0.30	3.00	0.002 325	0.34	2.60	0.001 530
0.27	2.20	0.003 463	0.31	1.80	0.001 608	0.34	2.70	0.001 417
0.27	2.30	0.003 706	0.31	1.90	0.001 418	0.34	2.80	0.001 336
0.27	2.40	0.003 948	0.31	2.00	0.001 293	0.34	2.90	0.001 281
0.27	2.50	0.004 188	0.31	2.10	0.001 220	0.34	3.00	0.001 250
0.27	2.60	0.004 424	0.31	2.20	0.001 190	0.34	3.10	0.001 239
0.27	2.70	0.004 656	0.31	2.30	0.001 194	0.35	1.80	0.005 981
0.27	2.80	0.004 884	0.31	2.40	0.001 227	0.35	1.90	0.005 125
0.27	2.90	0.005 107	0.31	2.50	0.001 282	0.35	2.00	0.004 407
0.27	3.00	0.005 325	0.31	2.60	0.001 357	0.35	2.10	0.003 803
0.28	1.80	0.001 720	0.31	2.70	0.001 446	0.35	2.20	0.003 298
0.28	1.90	0.001 871	0.31	2.80	0.001 549	0.35	2.30	0.002 876
0.28	2.00	0.002 043	0.31	2.90	0.001 660	0.35	2.40	0.002 525
0.28	2.10	0.002 231	0.31	3.00	0.001 774	0.35	2.50	0.002 235
0.28	2.20	0.002 430	0.32	1.80	0.002 257	0.35	2.60	0.001 997
0.28	2.30	0.002 637	0.32	1.90	0.001 922	0.35	2.70	0.001 802
0.28	2.40	0.002 849	0.32	2.00	0.001 668	0.35	2.80	0.001 645
0.28	2.50	0.003 063	0.32	2.10	0.001 482	0.35	2.90	0.001 521
0.28	2.60	0.003 274	0.32	2.20	0.001 348	0.35	3.00	0.001 426
0.28	2.70	0.003 482	0.32	2.30	0.001 260	0.36	1.80	0.007 748
0.28	2.80	0.003 689	0.32	2.40	0.001 210	0.36	1.90	0.006 698
0.28	2.90	0.003 894	0.32	2.50	0.001 191	0.36	2.00	0.005 805
0.28	3.00	0.004 096	0.32	2.60	0.001 198	0.36	2.10	0.005 044
0.29	1.80	0.001 320	0.32	2.70	0.001 226	0.36	2.20	0.004 397
0.29	1.90	0.001 375	0.32	2.80	0.001 273	0.36	2.30	0.003 846
0.29	2.00	0.001 463	0.32	2.90	0.001 335	0.36	2.40	0.003 378
0.29	2.10	0.001 578	0.32	3.00	0.001 409	0.36	2.50	0.002 980
0.29	2.20	0.001 713	0.33	1.80	0.003 215	0.36	2.60	0.002 645
0.29	2.30	0.001 863	0.33	1.90	0.002 718	0.36	2.70	0.002 363
0.29	2.40	0.002 025	0.33	2.00	0.002 320	0.36	2.80	0.002 126
0.29	2.50	0.002 195	0.33	2.10	0.002 005	0.36	2.90	0.001 931
0.29	2.60	0.002 371	0.33	2.20	0.001 758	0.36	3.00	0.001 769

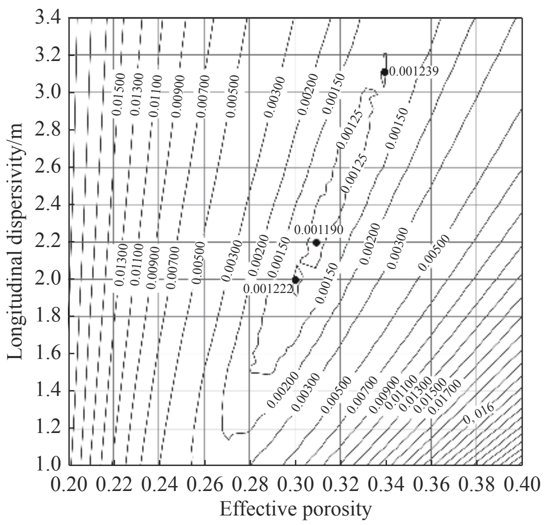

Fig. 11 The average least squares and corresponding effective porosity and longitudinal dispersivity

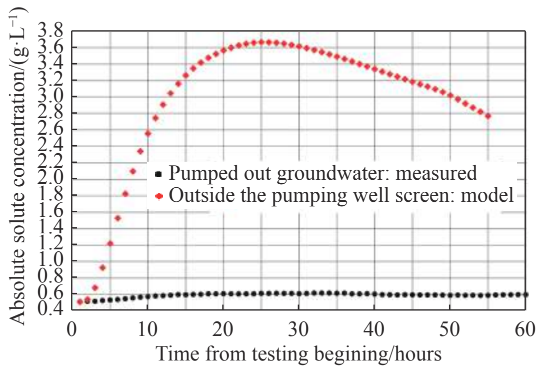

Fig. 12 Absolute solute concentration in the pumped GW and outside the pumping well screen corresponding to the minimal least squares

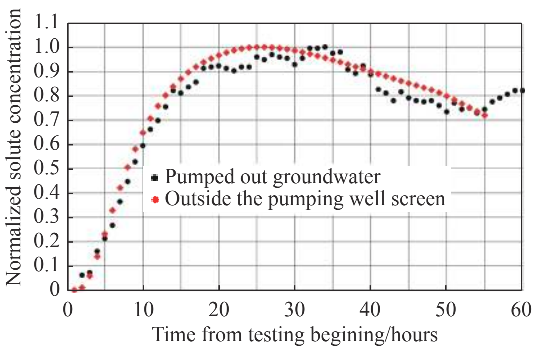

Fig. 13 Normalized solute concentration in the pumped GW and outside the pumping well screen corresponding to the minimal least squares

so-called scale-dependence of longitudinal dispersivity, i.e. dispersivity increases with the scale of test (the distance between the tracer injection and observation wells) as Gelhar et al. (1992) have found based on the analysis of 59 different field sites.

The parameters uncertainty may be also from the error of the numerical modelling due to the temporal and spatial discretization. Meanwhile, the parameter identification deals with two unknown parameter variables, i.e. effective porosity and dispersivity, in one advection-dispersion differential equation, in which a dispersion term contains a ratio of dispersivity to effective porosity, and an advection term contains effective porosity. The sensitivity of the two terms in the resulted tracer transport and possible numerical modelling error would provide an identified ratio of dispersivity to effective porosity and a set of the two parameters. This phenomenon would be seen from Fig. 11 the sets of porosity and dispersivity would be from 0.30 m and 2.0 m to 3.4 m and 3.1 m with the squared errors of from 0.001 190 to 0.001 239.

3 Discussions

Through the interpretation of the GW tracer injection testing data and analysis of the solute transport parameters of the sub-aquifer qp_1 in the southern part of Hanoi city, the following discussions can be addressed:

-In accordance with Fetter (2001), the total porosity of well sorted gravels is in the range 0.25-0.50 and that of the gravels is 0.20-0.35. For the sands, gravels and pebbles, the effective porosity is almost the same as the total porosity (Fetter, 2001) since there are almost no dead-end pores in such loose formation (Bear and Verruijt, 1987). Therefore, the identified effective porosity equal to 0.31 obtained in this work is within the possible porosity range for sands, gravels and pebbles of the sub-aquifer qp_1, without any contradiction. This value is well comparative with the value presented by Zhu et al. (2018) for sandy soil northwest of Laixi in Shandong Province, China.

-During the tracer injection, some instabilities of the injection (variable injection rates or even with some discontinuity of injection) did occur. The effective porosity may be calculated through such discontinuity points along with other relevant parameters (pumping rate, aquifer thickness and distance between the pumping and injection wells). However, for incompletely single confined aquifer (for example, for leaky confined aquifer), such application definitely produces errors and inaccuracies. A careful pumping data interpretation and analysis need to be carried out in order to apply the effective porosity determination in an appropriate way.

-The identified longitudinal dispersivity value of

2.20 m for the sub-aquifer qp_1 is a rather high value compared to the characteristic grain size of the aquifer (Bear and Verruijt, 1987), i.e. the longitudinal dispersivity is an order of the characteristic grain size. However, in the practice, there are lots of experimental data showing this large value trend of the longitudinal dispersivity. This obtained longitudinal dispersivity value is even smaller than 10-15 m which were used by Zhu et al. (2018) for sandy soil northwest of Laixi in Shandong Province, China.

-The flow distortion coefficient α_w is an important parameter in the data interpretation and analysis of GW solute transport parameters and plays an important role in the efficiency of the tracer injection testing. Therefore, appropriate drilling and GW well construction technique should be used to ensure the maximal well efficiency.

4 Conclusions

The study has proposed an adaptive way to analyze tracer injection-withdrawal testing data to identify both effective porosity and longitudinal dispersivity of non-adsorptive aquifers. The proposed methodology uses only one-dimensional numerical modelling and had been shown to be successful in the application to a real field testing data. The methodology may overcome some required strict constraints in injection-withdrawal models, such as the steady state flow condition and constant continuous tracer injection, and also in more sophisticated two- or three-dimensional models which would require more parameter-variables such as transverse dispersivity in vertical and horizontal perpendicular to the radial direction. The methodology may cope with some convenient issues such as only solute concentration of pumped GW is measured, the injection rate and tracer concentration of injected fluid would accidentally be changed (but need to be recorded) etc.

To ensure the accuracy of parameter identification, reliable testing data during a tracer injection-withdrawal testing and to deal with the parameter identification uncertainty, the following is recommended: 1) A stable solute injection in term of solute concentration and injection rate to ensure a smooth temporal concentration without any further data processing which may bring some inaccuracy; 2) Some solute monitoring wells along the section line connecting the pumping and injection wells are recommended to be installed to monitor the solute concentration outside the well's screen; 3) Exact estimates of the aquifer thickness and leakage parameters of the aquifer are required in order to be able to analytically determine the effective porosity; 4) Constant pumping and injection rates to ensure a stable velocity field over the entire testing time; 5) Maximal well efficiency of the tracer injection well should be achieved to ensure an efficient use of tracer and an accuracy of tracer analysis.

References

Barone FS, Rowe RK, Quigley RM. 1992. A laboratory estimation of diffusion and adsorption coefficients for several volatile organics in natural clayey soils. Journal of Contaminant Hydrology, 10(3): 225-250.

Bear J, Verruijt A. 1987. Modeling groundwater flow and pollution. D Reidel Publishing Company, Dordrecht: Holland.

Brouyère S. 2003. Modeling tracer injection and well-aquifer interactions: A new mathematical and numerical approach. Water Resource Research, 39(3): 1070-1075.

Do Van Binh. 2013. Source and formation of the arsenic in ground water in Hanoi, Vietnam. Journal of Groundwater Science and Engineering, 1(1): 102-108.

Dong P. 1998. Mathematical modelling of coastal processes. Proceedings of the Forty Ninth Scottish Universities “Physical processes in the Coastal Zone: Computer modelling and remote sensing”. 95-108.

Drost W, Klotz D, Koch A et al. 1968. Point dilution methods of investigating ground water flow by means of radioisotopes. Water Resource Research, 4(1): 125-146.

Fetter CW. 2001. Applied Hydrogeology. Prentice Hall Inc. New Jersey 07458.

Fried JJ. 1975. Groundwater pollution: Theory, methodology, modelling, and practical rules. Elsevier Scientific Publishing Company. 330.

Gelhar LW, Welty C, Rehfeldt KR. 1992. A critical review of data on field-scale dispersion in aquifers. Water Resource Research, 28(7): 1955-1975.

Glen BC, Welty C, Buxton HT. 1999. Design and analysis of tracer tests to determine effective porosity and dispersivity in fractured sedimentary rocks, Newark basin, New Jersey. US Geological Survey. Water-Resources Investigations Report 98-4126A.

Gutierrez A, Klinka T, Thiery D, et al. 2013. TRAC, a collaborative computer tool for tracer-test interpretation. EPJ Web of Conferences 50: 03002.

Hall SH. 1996. Practical single-well tracer methods for aquifer testing. In: Tenth National Outdoor Action Conference and Exposition, National Groundwater Association, Columbus, Ohio, USA, 11.

Honjo Y, Sato K, Nguyen Van Hoang. 1997. Groundwater of Hanoi, Vietnam: Parameter identification by the Bayesian method. Proceedings of Theme C: Groundwater: An Endangered Resource (463-468), the 27th IAHR Congress California, USA.

Huyakorn PS, Pinder GF. 1983. Computational methods in subsurface flow. Academic Press, New York: 473.

Keisuke K, Takeshi H, An Thuan Do, et al. 2017. Groundwater recharge in suburban areas of Hanoi, Vietnam: Effect of decreasing surface-water bodies and land-use change. Hydrogeology Journal, 25: 727-742.

Klotz D, Seiler K P, Moser H. 1980. Dispersivity and velocity relationship from laboratory and field experiments. Journal of Hydrology, 45(4): 169-184.

Martyna G, Emiliano S, Daniel S, et al. 2021. Arsenic behavior in groundwater in Hanoi (Vietnam) influenced by a complex biogeochemical network of iron, methane, and sulfur cycling. Journal of Hazardous Materials, 407(5).

Nguyen Van Hoang. 2018. Study on the finite element modeling software for simulation of groundwater flow and solute transport by groundwater-application to aquifer in central plain of Vietnam. Codded ĐT. NCCB-ĐHƯD. 2012-G/04 supported by NAFOSTED-MOST.

Novakowski KS. 1992. An evaluation of boundary conditions for one-dimensional solute transport: 1-Mathematical development. Water Resource Research, 28(9): 2399-2410.

Rifai MNE, Kaufman WJ, Todd DK. 1956. Dispersion phenomena in laminar flow through porous media. Sanitary Engineering Research Laboratory and Division of Civil Engineering, University of California, 93(2): 157.

Sharma PK, Sawant VA, Shukla SK, et al. 2014. Experimental and numerical simulation of contaminant transport through layered soil. International Journal of Geotechnical Engineering, 8(4): 345-351.

Shook GM, Ansley SL, Wylie A. 2004. Tracers and Tracer Testing: Design, Implementation, and Interpretation Methods. US Department of Energy Office of Environmental Management. Report NEEL/EXT-03-01466.

Welty C, Gelhar LW. 1994. Evaluation of longitudinal dispersivity from non-uniform flow tracer tests. Journal of Hydrology, 153(1): 71-102.

Yan X, Qian J, Ma L. 2019. Experimental study on the velocity-dependent dispersion of the solute transport in different porous media. Journal of Groundwater Science and Engineering, 7(2): 106-114.

Zhou L. 2002. Solute transport in layered and heterogeneous soils. Louisiana State University and Agricultural and Mechanical College. Ph. D. Thesis.

Zhu H, Jia C, Xu Y, et al. 2018. Study on numerical simulation of organic pollutant transport in groundwater northwest of Laixi. Journal of Groundwater Science and Engineering, 6(4): 106-1114.

Zienkiewicz OC, Morgan K. 1983. Finite Elements and Approximation. Academic Press.

Zlotnik VA, Logan J D. 1996. Boundary Conditions for Convergent Radial Tracer Tests and Effect of Well Bore Mixing Volume. Papers in the Earth and Atmospheric Sciences: 159.